



Common-Reflection-Surface stack – a generalized stacking velocity analysis tool

Jürgen Mann, Geophysical Institute, University of Karlsruhe, Germany

Copyright 2005, SBGf – Sociedade Brasileira de Geofísica

This paper was prepared for presentation at the 9th International Congress of The Brazilian Geophysical Society held in Salvador, Brazil, September 11-14 2005.

Contents of this paper was reviewed by The Technical Committee of the 9th International Congress of The Brazilian Geophysical Society and does not necessarily represent any position of the SBGf, its officers or members. Electronic reproduction, or storage of any part of this paper for commercial purposes without the written consent of The Brazilian Geophysical Society is prohibited.

Summary

The Common-Reflection-Surface (CRS) stack has originally been considered as an alternative stacking tool to simulate high quality zero-offset section from seismic multi-coverage data. Meanwhile, this perception has significantly changed in favor of the stacking parameters employed in the CRS stack. The fully automated determination of these parameters during the CRS stack can be seen as generalization of the well established stacking velocity analysis applied in the conventional NMO/DMO/stack approach. As the CRS stack accounts for local dip and curvature of reflectors in depth, its stacking parameters carry far more information about the subsurface than conventional stacking velocity. Consequently, applications based on such stacking parameters, e. g., velocity model determination, directly benefit from this generalization: more stable results can be achieved in a more automated manner with less rigorous constraints compared to conventional methods.

I briefly review the basic concepts of the CRS stack method and illustrate them with a data example. The main message is that this method facilitates various imaging problems, e. g., inversion, depth imaging, and automated horizon picking.

Introduction

Conventional stacking velocity analysis is performed in certain subsets of seismic multi-coverage data, namely in common-midpoint (CMP) gathers. The stacking velocity v_{stack} is usually considered as an effective velocity of a reflector's overburden suited to approximate the CMP traveltime up to second order in source/receiver offset. Figures 1a and b show that the stacking trajectory in the CMP gather clearly deviates from the trajectory related to a single reflection point, the so-called Common-Reflection-Point (CRP) trajectory. In other words, different reflection points contribute to v_{stack} which, thus, also depends on reflector properties like dip and curvature, although the latter can be neglected in the considered second-order approximation.

The inherent mixing of properties of the reflector and its overburden during velocity analysis is commonly resolved by means of a sequence normal moveout(NMO)/dip moveout(DMO)/stack. As NMO velocities are not directly available from stacking velocity analysis, this involves various additional approximations and multiple velocity analyses

and moveout corrections. NMO/DMO/stack can be seen as an approximation of a migration to zero-offset (MZO) which collects all information related to potential reflection points located on the ZO isochron defined by ZO traveltime t_0 (see Figure 1c). DMO correction removes the dip dependence of v_{stack} , at this stage often called DMO velocity, but does not provide additional stacking parameters characterizing the subsurface.

For laterally inhomogeneous models, there is no good reason to restrict stacking velocity analysis with its above-mentioned drawbacks to CMP gathers, only. Instead of searching for CMP stacking trajectories, i. e., curves in the prestack data volume, it is more appropriate to approximate the spatial reflection events present in the multi-coverage data by *spatial* stacking operators from the very beginning. This is where the concepts of the CRS stack come into play: it is based on the kinematic reflection response of a reflector segment with arbitrary dip and curvature. In other words, reflector properties are considered up to second order. The spatial CRS stacking operator (see Figure 1d) involves an entire set of stacking parameters, often also called kinematic wavefield attributes, which ensure a sufficient degree of freedom to account for the properties of the overburden *and* the reflector in a separable way. As a consequence, the CRS wavefield attributes provide more information about the subsurface. NMO/DMO specific assumptions like plane or even horizontal reflectors can be entirely avoided.

CRS traveltime approximation

The CRS stacking operator can be derived in different ways, e. g., by means of paraxial ray theory (Schleicher et al., 1993) or by means of geometrical optics (Höcht et al., 1999). It is convenient to use midpoint and half-offset coordinates

$$\mathbf{x}_m = \frac{1}{2}(\mathbf{x}_g + \mathbf{x}_s) \quad \text{and} \quad \mathbf{h} = \frac{1}{2}(\mathbf{x}_g - \mathbf{x}_s),$$

where the two-dimensional vectors \mathbf{x}_s and \mathbf{x}_g denote the shot and receiver locations, respectively. To quickly enter into the matter, we can start with a very pragmatic approach: we are looking for a second-order approximation of reflection traveltimes. Let us assume that one point $(t, \mathbf{x}_0, \mathbf{h}_0)$ on a reflection event is already known, where t denotes traveltime. The simplest idea is to expand the reflection event in terms of a Taylor series. Although the CRS operator can also be expressed for finite offsets (see, e. g., Zhang et al., 2001), I will only consider the zero-offset (ZO) case $\mathbf{h}_0 = \mathbf{0}$ with normal incidence of the ZO ray on the reflector in the following. This is the same restriction inherent to conventional stacking velocity analysis and implies that all first derivatives with respect to any component of \mathbf{h} van-

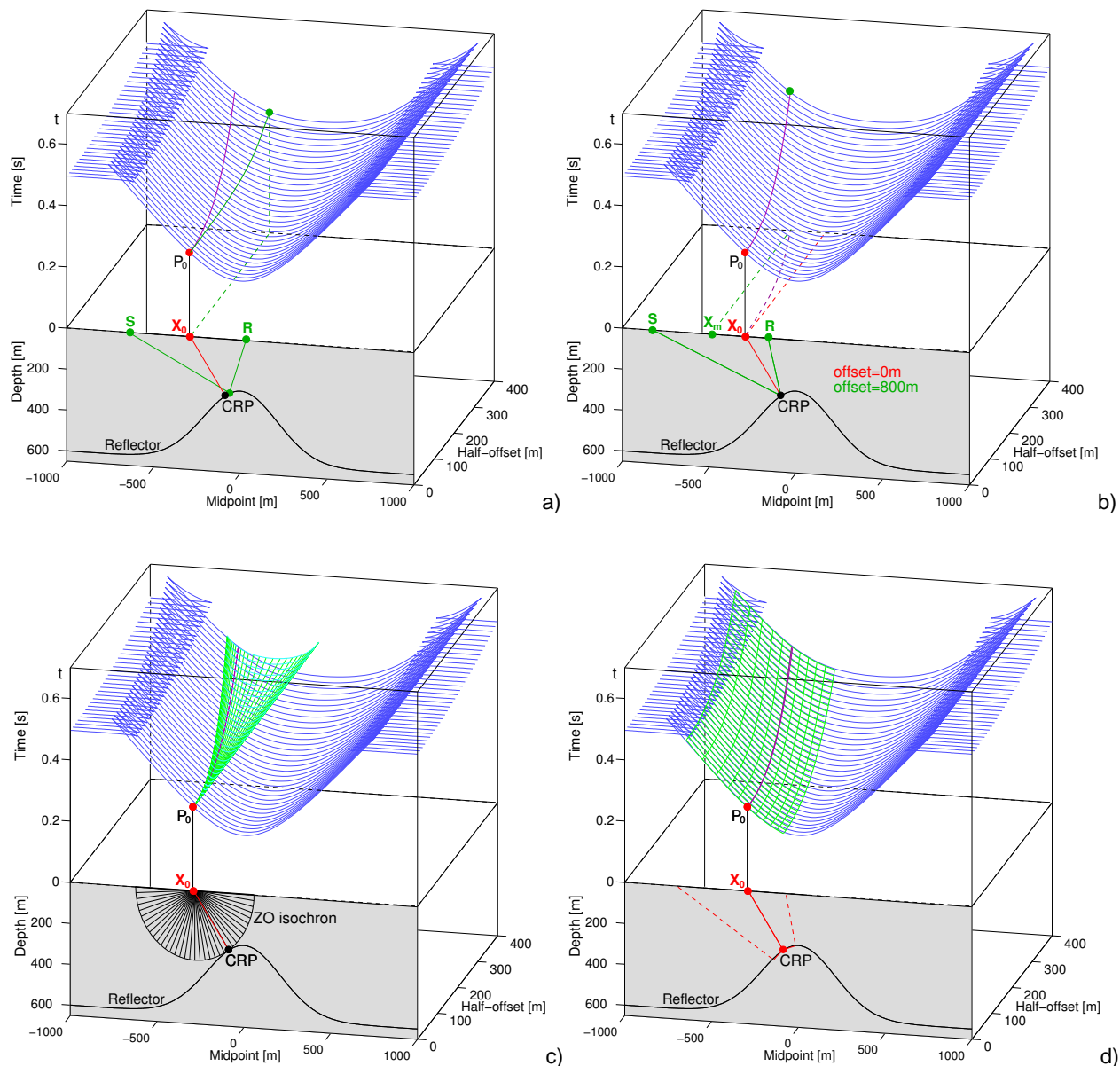


Figure 1: Stacking operators of different stacking approaches for a simple 2D model with homogeneous overburden: a) NMO/stack approach (physical model only for 1D case), b) CRP stack based on single reflection point in depth, c) MZO (commonly approximated by the sequence NMO/DMO/stack) based on reflection response of the ZO isochron, d) CRS operator based on a reflector segment with arbitrary dip and curvature. The operators in subfigures b-d are set up by means of CRP trajectories, the magenta line represents the optimum stacking operator, i. e., the CRP trajectory for the chosen depth point. The stacking operators are shown in green, the forward-calculated traveltimes in blue. The upper parts of the cubes represent the prestack time domain (x_m, h, t) , the lower parts the 2D depth domain (x, z) .

ish. In this case, the Taylor series reduces to

$$t(\mathbf{x}_m, \mathbf{h}) = t_0 + 2 \mathbf{p}_m \cdot (\mathbf{x}_m - \mathbf{x}_0) + (\mathbf{x}_m - \mathbf{x}_0)^T \mathbf{M}_m (\mathbf{x}_m - \mathbf{x}_0) + \mathbf{h}^T \mathbf{M}_h \mathbf{h}, \quad (1)$$

with the spatial traveltimes derivatives $\mathbf{p}_m = \frac{1}{2} \partial t / \partial \mathbf{x}_m$, $\mathbf{M}_m = \frac{1}{2} \partial^2 t / \partial \mathbf{x}_m^2$, and $\mathbf{M}_h = \frac{1}{2} \partial^2 t / \partial \mathbf{h}^2$ evaluated with respect to all vector components at $(\mathbf{x}_0, \mathbf{h}_0) = \mathbf{0}$. A more familiar hyperbolic representation can be obtained by using a second-order approximation of t^2 rather than t .

Kinematic wavefield attributes

So far, there are no assumptions concerning homogeneity and isotropy. To allow for a geometrical interpretation of the traveltimes derivatives, I will now assume a isotropic near-surface with a locally constant velocity v_0 . The vector \mathbf{p}_m specifies the emergence direction (emergence angle α and azimuth ϕ) of the normal ray emerging at \mathbf{x}_0 : $\mathbf{p}_m = \left(v_0^{-1} \sin \alpha \cos \phi, v_0^{-1} \sin \alpha \sin \phi \right)^T$.

Let us now consider the ZO case $\mathbf{h} = \mathbf{0}$. It is well known

that ZO modeling can be performed by means of exploding reflector experiments. Indeed, the symmetric matrix of derivatives \mathbf{M}_m can be directly related to the curvature \mathbf{K}_N of a wavefront due to such an exploding reflector experiment, also called normal wave: $\mathbf{M}_m = v_0^{-1} \mathbf{TK}_N \mathbf{T}^T$. Here, \mathbf{T} is the 2×2 upper left submatrix of the transformation matrix from the ray-centered to the global Cartesian coordinate system.

Matrix \mathbf{M}_h describes the second traveltime derivatives in the CMP configuration $\mathbf{x}_m = \mathbf{0}$. Hubral and Krey (1980) showed that in second-order approximation, the CMP traveltimes coincide with ZO traveltimes of diffractor located at the normal incidence point (NIP) of the normal ray. Thus, \mathbf{M}_h can be related to the curvature \mathbf{K}_{NIP} of a wavefront caused by a exploding reflection point experiment, the so-called NIP wave: $\mathbf{M}_h = v_0^{-1} \mathbf{TK}_{\text{NIP}} \mathbf{T}^T$. Alternatively, \mathbf{K}_N and \mathbf{K}_{NIP} can be defined by means of two-way experiments, so-called eigenwaves, which either impinge normally to the reflector or focus in the NIP, respectively.

Degrees of freedom

With the kinematic wavefield attributes \mathbf{p}_m , \mathbf{K}_N , and \mathbf{K}_{NIP} the CRS operator (1) can now be entirely expressed in terms of the curvatures of the NIP and normal wavefront at \mathbf{x}_0 and their common propagation direction. It is evident that \mathbf{K}_N carries information about the reflector curvature, whereas \mathbf{K}_{NIP} only carries information about the overburden encountered along the normal ray. Let us compare the number of parameters defined in the depth domain and at the acquisition surface and in the time domain: to locally characterize a reflector segment in depth, we need its location (x, y, z) , its dip and azimuth (δ, θ) , and its curvature given by a symmetric matrix \mathbf{K}_R . Thus, we have a total of eight parameters. The corresponding reflection event is locally parameterized by ZO traveltime t_0 , the emergence location \mathbf{x}_0 and direction (α, ϕ) of the normal ray, as well as the symmetric curvature matrices \mathbf{K}_N and \mathbf{K}_{NIP} , yielding a total of 11 parameters. Obviously, we have three independent parameters that remain to characterize the overburden along the central ray. This might, e.g., be expressed as an azimuth-dependent effective velocity of the overburden. In case of 2D acquisition, the numbers of parameters reduces to four vs. five, corresponding to the fact that no azimuth dependence has to be handled in 2D.

Generalized stacking velocity analysis

Similar to a conventional stacking velocity analysis, the kinematic wavefield attributes have to be determined directly from the multi-coverage data by means of coherence analyses. As the CRS stacking operator (1) is not restricted to the CMP configuration, it defines a four-dimensional hyper-surface in the five-dimensional data hyper-volume spanned by time t , the half-offset vector \mathbf{h} , and the midpoint vector \mathbf{x}_m . This might explain why Figure 1 only illustrates the case of 2D data acquisition.

During the coherence analysis, not only a in general azimuth dependent stacking velocity has to be determined but an entire set of eight attributes. To achieve an acceptable computational efficiency, this global optimization problem can be split into separate optimizations performed in subsets of the data with a reduced number of parameters in each search step. Details on such search strategies can, e.g., be found in Mann (2002), Müller (2003), and Bergler (2004).

In view of the many dimensions of the optimization problem, a manual velocity picking is impractical. Therefore, the CRS stack is usually applied in an automated high-density manner such that the optimum stacking operator and its eight parameters are determined separately for each ZO (t_0, \mathbf{x}_0) location to be considered.

Summarizing the preceding paragraphs, the CRS stack might be described as an generalized, multi-dimensional, multi-parameter, high-density stacking velocity analysis.

3D data example and application of attributes

In the 3D case, the CRS stack not only provides a simulated ZO volume of high signal/noise ratio, but also a volume of each of the eight kinematic wavefield attributes. In addition, the coherence values calculated along the optimum stacking operators set up a coherence volume which allows to identify reflection events and to evaluate the reliability of their associated wavefield attributes. This is crucial for the removal of unphysical outliers and fluctuations in the attribute volumes as they usually occur in high-density velocity analysis: as discussed by Mann and Duvencek (2004), the wavefield attributes identified as being reliable allow an event-consistent smoothing of the attributes which cannot be achieved with conventional approaches in such an easy and consistent way. Furthermore, similar concepts can be employed for the automated picking of reflection events and their associated wavefield attributes.

To illustrate the vast amount of information determined by the CRS stack, it has been applied to a synthetic 3D data set. Of course, it is impossible to present all ten data volumes mentioned above. Therefore, Figure 2 shows only sections extracted from a few of the results, namely an inline section of the stack volume and a crossline section of the coherence volume. Two of the eight wavefield attributes are depicted along automatically picked horizons: the inline radius of curvature of the NIP wavefront and the emergence angle of the normal ray. These two attributes, together with the azimuth ϕ of the normal ray (not display), are, e.g., suited to determine a smooth macro-velocity model for depth imaging by means of the so-called NIP-wave tomography (see, e.g., Duvencek, 2004).

The CRS attributes can even be of use in depth imaging: they allow to determine the stationary point for Kirchhoff migration and to estimated the size of the projected Fresnel zone for ZO, together defining the optimum, minimum migration aperture for ZO. Jäger (2005) additionally extrapolated the stationary point to finite offsets along the approximate CRP trajectory. This lead to a CRS-based limited-aperture Kirchhoff prestack and poststack depth migration.

Conclusions

The CRS stack approach has been described in terms of a generalized, multi-dimensional, multi-parameter, high density stacking velocity analysis. It naturally accounts for subsurface properties like reflector dip and curvature and, thus, provides far more degrees of freedom to parameterize reflectors as well as their overburden compared to conventional stacking velocity.

I have briefly discussed the theoretical background of CRS stack and various implications of this more general approach to different imaging and inversion tasks, like velocity model determination or minimum-aperture migration.

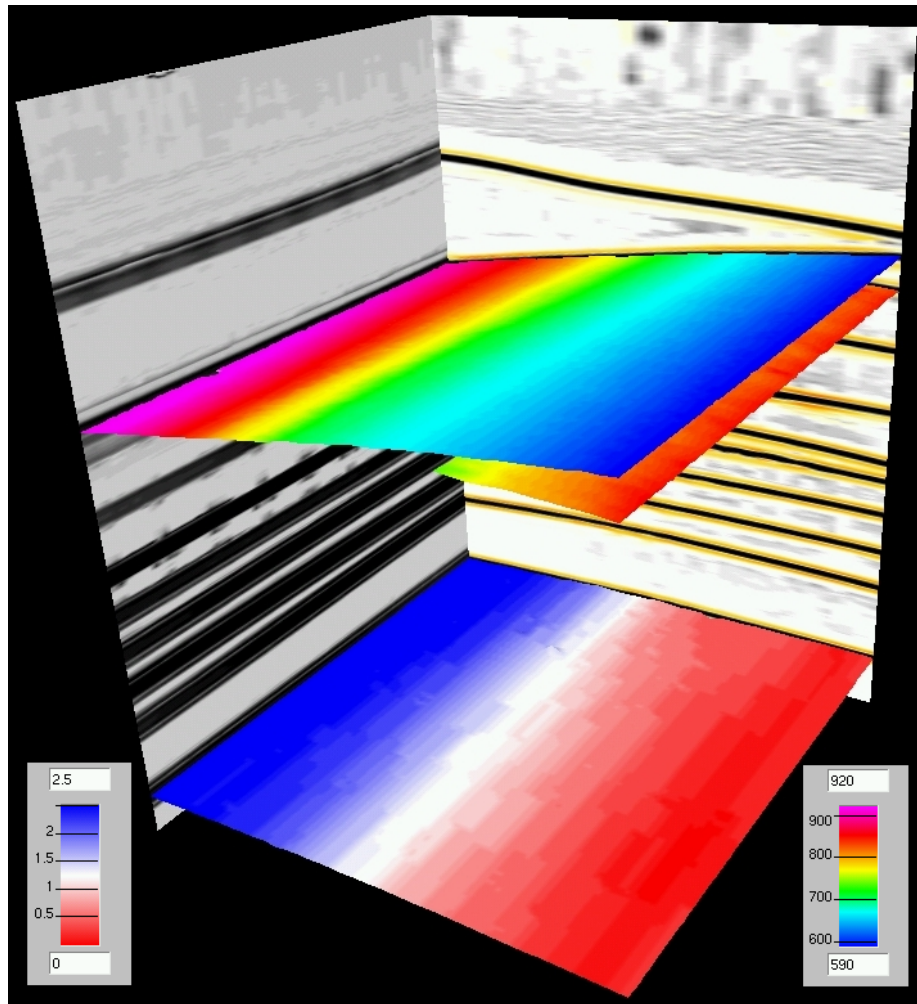


Figure 2: Some of the CRS results obtained for a synthetic 3D data set: an inline section extracted from the simulated 3D ZO volume (right), a coherence section extracted along a cross line (left, black indicates high coherence values). CRS attributes extracted from the attribute volumes along automatically picked horizons: inline radius of curvature [m] of the NIP wavefront (top, right hand legend), emergence angle [°] of the normal ray (bottom, left hand legend).

Acknowledgments

I would like to thank the sponsors of the Wave Inversion Technology (WIT) Consortium and the Brazilian Geophysical Society for their support. I am obliged to all colleagues who contributed to this work, especially Tilman Klüver and Thomas Hertweck.

References

- Bergler, S. (2004). *On the determination and use of kinematic wavefield attributes for 3D seismic imaging*. Logos Verlag, Berlin.
- Duveneck, E. (2004). Velocity model estimation with data-derived wavefront attributes. *Geophysics*, 69(1):265–274.
- Höcht, G., de Bazelaire, E., Majer, P., and Hubral, P. (1999). Seismics and optics: hyperbolae and curvatures. *J. Appl. Geophys.*, 42(3,4):261–281.
- Hubral, P. and Krey, T. (1980). *Interval velocities from seismic reflection traveltimes measurements*. Soc. Expl. Geophys., Tulsa.
- Jäger, C. (2005). Minimum-aperture Kirchhoff migration by means of CRS attributes. In *Extended abstracts, 67th Conf. Eur. Assn. Geosci. Eng. Session F042*.
- Mann, J. (2002). *Extensions and applications of the Common-Reflection-Surface Stack method*. Logos Verlag, Berlin.
- Mann, J. and Duveneck, E. (2004). Event-consistent smoothing in generalized high-density velocity analysis. In *Expanded Abstracts, 74th Ann. Internat. Mtg. Soc. Expl. Geophys. Session ST 1.1*.
- Müller, A. (2003). *The 3D Common-Reflection-Surface stack – theory and application*. Master's thesis, University of Karlsruhe.
- Schleicher, J., Tygel, M., and Hubral, P. (1993). Parabolic and hyperbolic paraxial two-point traveltimes in 3D media. *Geophys. Prosp.*, 41(4):495–514.
- Zhang, Y., Bergler, S., and Hubral, P. (2001). Common-Reflection-Surface (CRS) stack for common-offset. *Geophys. Prosp.*, 49(6):709–718.